Surface characterization of 1-butyl-1-ethylpiperidinium bromide by inverse gas chromatography

Stella Papadopoulou, Nicolas Papaiconomou, Stephane Baup, Cristina Iojoiu, Lenka Svecova, Pierre-Xavier Thivel

Surface characterization of 1-butyl-1-ethylpiperidinium bromide by inverse gas chromatography

Stella K. Papadopoulou[a,*], Nicolas Papaiconomou[a,b], Stéphane Baup[c], Cristina Iojoiu[a], Lenka Svecova[a], Pierre-Xavier Thivel[a]

[a] *Université Grenoble Alpes, Université Savoie Mont Blanc, CNRS, Grenoble INP, LEPMI, 38000 Grenoble, France*

[b] *Institut de Chimie de Nice, Université Côte d'Azur, UMR CNRS 7272, Parc Valrose, F-06108 Nice Cedex 2, France*

[c] *Université Grenoble Alpes, CNRS, Grenoble INP, LRP, 38000 Grenoble, France*

* Corresponding author e-mail address: papadopoulou.styliani@gmail.com (S.K Papadopoulou)

Abstract

This work addresses the surface characterization of an organic salt based on a piperidinium cation and a halide anion, similar to a first generation ionic liquid, using the Inverse Gas Chromatography (IGC) technique. IGC was employed in order to assess the dispersive surface energy and the acid/base character of 1-butyl-1-ethylpiperidinium bromide, $[C_2C_4PIP]Br$ at a temperature range (313.15-343.15 K) well below its melting point, where the retention mechanism is governed by the surface adsorption of the probes. This type of characterization was possible due to the high melting point of $[C_2C_4PIP]Br$, namely 413.15 K. The dispersive component of the surface energy was estimated with the aid of the Schultz method and the Dorris-Gray method. Results obtained using the first method were higher than the ones obtained by the latter. The discrepancy between the two methods was found to increase with the increase of temperature. The acid/base characterization was implemented by using the Flour and Papirer approach as well as the Brookman and Sawyer method. The acidity and basicity constants of the surface of $[C_2C_4PIP]Br$ revealed that it is amphoteric with a predominantly basic character.

Keywords: Ionic liquids; Inverse gas chromatography; 1-butyl-1-ethylpiperidinium bromide; Surface energy; Acid-base interactions

1 Introduction

Ionic liquids (ILs) are salts exhibiting low melting points, typically below 100°C, composed of anions and large organic cations, such as imidazolium, pyridinium, pyrrolidinium and less commonly piperidinium [1-6]. ILs have a number of interesting properties such as non-volatility, non-flammability, high thermal and ionic conductivity and an enhanced solvation ability for a wide range of materials [1, 4, 5, 7]. On these grounds, ILs have been widely explored as 'green' media in chemical and catalytic reactions, distillations, liquid-liquid extractions and solvent-aided crystallizations [1, 4, 5]. Other studies report the utilization of ILs as lubricants, in gas separation processes and as gas storage media [7]. ILs were also employed as electrolytes in batteries, electrochemical capacitors [3] and as catalysts [8].

Piperidinium based ILs are of special interest for electrochemical applications due to their water immiscibility, high conductivities and wide electrochemical windows [9, 10]. As piperidinium based ionic liquids contain only saturated carbons, Shukla demonstrated that for a given anion, these ILs exhibit higher melting points and are thermally more stable than the respective imidazolium ILs having the same alkyl chains appended on the cation [9, 10]. In particular, piperidinium bromide salts exhibit very high melting points (in the vicinity of 200°C) whereas their homologous imidazolium bromide salts are either liquids or present low melting points [9, 10]. When ionic liquids are involved in applications such as extraction and catalysis, the presence of a second phase (liquid of gas) other than the ionic liquid is required. Reactions, interactions and chemical exchanges that take place at the interface of the two-phase systems strongly depend on the surface properties of each fluid [11]. Therefore, the understanding of surface related properties of ionic liquids, such as their surface energy and acid-base character is necessary for the elucidation of the mechanisms that govern these reactions [7, 12-15].

Although there is a plethora of experimental studies investigating the surface tension of ionic liquids with various techniques [16], only a restricted number of publications address the estimation of the dispersive surface energy of ionic liquids with the use of inverse gas chromatography (IGC). Over the past years, inverse gas chromatography has proved to be a valuable tool towards the characterization of the surface and thermodynamic properties of various inorganic and organic materials such as polymers, fillers and pharmaceuticals [17]. It should be outlined that the choice of the measurement temperature range is crucial in IGC as

it determines the state (melt or solid) of the material under study, governing thus the retention mechanism of the probes (surface adsorption in the case of solids or mixing with bulk of the melt) [17].

Although during the last decade IGC appears to be very popular for the thermodynamic characterization of ionic liquids [8, 18-26], it has rarely been utilized for their surface characterization. This is due to the fact that such characterization should be conducted at a temperature range below the melting point of the IL in order to ensure that the interaction mechanism between the probes and IL is surface adsorption [17]. On these grounds, as ILs exhibit low melting points, IGC is rather appropriate for the surface analysis of high melting point salts or for the thermodynamic characterization of ionic liquids.

The group of Wang has published a series of papers on the surface [27-29] and thermodynamic characterization [8, 18, 30-33] of methyl imidazolium ILs by means of IGC. To our knowledge, these are the only IGC studies addressing the surface characterization of ionic liquids [27-29]. It has to be stressed that the authors conducted both the surface and the thermodynamic characterizations at the same experimental temperature range, which is well above the melting point of the studied ILs [34]. Given the fact that the studied substances were in all cases in the liquid state and thus the probes' interaction mechanism was bulk absorption, the measurement temperatures used in these three studies were not appropriate for the surface characterization of the methyl imidazolium ILs.

In the current contribution, we present the results of the IGC surface characterization of 1-butyl-1-ethylpiperidinium bromide [C_2C_4PIP]Br. Piperidinium based ILs is a family of ionic liquids much less studied than those based on imidazolium or pyridinium cations for example [35]. Concerning their IGC characterizations, only a limited number of studies have reported the estimation of the thermodynamic properties of piperidinium-based ILs bearing anions other than the bromide anion, or with different alkyl chain appended onto the cation, as those present in [C_2C_4PIP]Br [36-38]. 1-butyl-1-ethylpiperidinium bromide is an organic salt being by all aspects similar to halide-based ionic liquid, with the exception that its melting point is above 373 K. Hence, IGC measurements were performed at 313.15-343.15 K, a temperature range which is below the melting point of [C_2C_4PIP]Br. The energy, enthalpy and entropy of adsorption of polar probes on the surface of the salt, the dispersive component of the surface energy and the Lewis acidity and basicity constants of [C_2C_4PIP]Br were determined. The dispersive interactions were investigated with the aid of well-known methods proposed by Dorris and Gray and by Schultz, whereas the specific interactions of the polar probes were calculated using the Brookman and Sawyer approach and the Flour and Papirer method.

In this article, after the theoretical background section and a section dedicated to detailing the procedure used for carrying out the IGC analysis, results will be presented and discussed.

2 Theoretical background

Contrary to the conventional gas chromatography, in IGC, the material under study is packed into the column where injections of carefully selected probes with known physicochemical properties are made [17, 39, 40]. The probes can be injected onto the column either at infinite dilution or at finite concentration. In the case of infinite dilution, the injection of minor amounts of the tested solvent makes sure that the retention is governed by the stationary phase-probe interactions and the probe-probe interactions are avoided [17].

The key measurement in IGC experiments is the net retention volume of the probes, V_N. It is expressed as the volume of the carrier gas necessary to elute the solute from the column and is calculated by the following equation [41]:

$$V_N = jF_M(t_R - t_M)\frac{T}{T_F}(1 - \frac{p_W}{p_0}) \quad (1)$$

where t_R, t_M are the probe's and marker's retention times, respectively, F_M is the carrier gas flow rate measured at the column outlet at ambient pressure, p_0 and at room temperature, T_F. Also, T is the column temperature, p_W is the vapor pressure of water at T_F and j is the James and Martin factor used to correct the gas carrier compressibility, defined as [41]:

$$j = \frac{3}{2}\left[\frac{\left(p_i/p_0\right)^2 - 1}{\left(p_i/p_0\right)^3 - 1}\right] \quad (2)$$

where p_i and p_0 are the column inlet and outlet pressures, respectively.

2.1 Dispersive interactions

The dispersive component of the surface energy of a solid, γ_s^d, can be determined, using the Dorris-Gray method [36], as described by the following equation:

$$\gamma_s^d = \left(\frac{1}{4\gamma_{CH_2}}\right)\left(\frac{-\Delta G^{CH_2}}{N\alpha_{CH_2}}\right)^2 \quad (3)$$

where ΔG^{CH_2} is the adsorption free energy of one methylene group, N is the Avogadro's number, α_{CH_2} is the cross-sectional area of an adsorbed methylene group (6 Å^2) and γ_{CH_2} is the surface free energy of a solid material constituted by methylene groups only, such as linear

polyethylene [$\gamma_{CH_2} = 35.6 - 0.058t$, with t being the working temperature, in °C)]. The adsorption free energy of one methylene group is calculated by the following equation:

$$\Delta G^{CH_2} = -RT \ln\left(\frac{V_{N(n+1)}}{V_{N(n)}}\right) \quad (4)$$

where $V_{N(n+1)}$ and $V_{N(n)}$ are the retention volumes of *n*-alkanes with n + 1 and n carbon atoms, respectively, T is the column temperature and R is the ideal gas constant. The slope of the straight line obtained by a plot of the surface free energy of adsorption of *n*-alkanes $RT \ln V_N$ versus the number of their carbon atoms is equal to the free energy of adsorption of a methylene group, ΔG^{CH_2}.

Another method used for the calculation of the dispersive component of the surface free energy, is the one proposed by Schultz et al. [42] and is based on the following equation:

$$-\Delta G_a = RT \ln V_N = 2N\alpha\sqrt{\gamma_s^d \gamma_l^d} + C \quad (5)$$

where α is the surface area of the probe molecules, γ_s^d and γ_l^d are the dispersive components of the surface energy of the solid and the liquid probe, respectively and C is a constant. γ_s^d can be extracted from the slope of the linear plot of the $RT \ln V_N$ values of *n*-alkanes versus the term $\alpha\sqrt{\gamma_l^d}$.

2.2 Specific interactions

The non-dispersive character of the stationary phase is studied by the employment of probes that can also interact through specific intermolecular forces with the stationary phase. When a polar probe is injected in the column, it interacts with the material under study by both dispersive and specific interactions. The term specific includes all types of interactions, i.e. polar, hydrogen bonding, metallic or magnetic, apart from the dispersive ones (London forces) [17]. Hence, the contribution of specific interactions to the free energy of adsorption, ΔG^{sp}, can be considered as the difference between the total free energy of adsorption, ΔG^{ads}, and the dispersive contribution to the free energy of adsorption ΔG^{d}. Several methods have been proposed for the determination of the ΔG^{sp} [17]. In the present study, ΔG^{sp} was calculated through the use of the Flour and Papirer approach [43] and the Brookman and Sawyer method [44]. The estimation of ΔG^{sp} is based on a plot of ΔG or simply $RT \ln V_n$ values of both polar and apolar probes versus their boiling temperatures (t_b, in °C) according to the Brookman and Sawyer method, or the $\log p^0$, logarithm of their saturated vapor pressure, according to the Flour and Papirer method. The *n*-alkane series leads to a linear plot,

which constitutes a reference straight line for the dispersive interactions. The contribution of specific interactions to the free energy of adsorption, ΔG^{sp}, corresponds to the vertical distance between the $-\Delta G^{ads}$ value and the reference line according to the equation:

$$(-\Delta G^{sp}) = (-\Delta G^{ads}) - (-\Delta G^{ref}) = RT \ln\left(V_N / V_{N,ref}\right) \quad (6)$$

where V_N is the net retention volume of the polar probe and $V_{N,ref}$ the net retention volume of a hypothetical alkane with the same boiling point or saturated vapor pressure as that of the polar probe.

The specific enthalpy, ΔH^{sp}, can be determined after the calculation of the specific component of the free energy of adsorption at various temperatures. When plotting the ΔG^{sp} values as a function of the reciprocal temperature, T^{-1}, ΔH^{sp} is calculated from the slope of the straight line corresponding to the following relation:

$$\Delta G^{sp}/T = \Delta H^{sp} \cdot 1/T - \Delta S^{sp} \quad (7)$$

The enthalpies of specific interactions between the examined surface and the polar probe can be used for the estimation of the K_A and K_B indices reflecting the acidity (electron acceptor) and basicity (electron donor) of a solid surface, respectively [17, 45-47] and are related to the acidic or basic character through the equation:

$$-\Delta H^{sp}/AN^* = K_A \cdot DN/AN^* + K_B \quad (8)$$

where DN [45] and AN^* [47] are Gutmann's donor and modified acceptor numbers of the polar probes, respectively. Hence, K_A and K_B can be determined by the slope and intercept, respectively, of the straight line obtained when plotting $\Delta H^{sp}/AN^*$ versus DN/AN^*. The K_B/K_A ratio provides an empirical basis for the classification of a surface with respect to acidity-basicity. At $K_B/K_A > 1$ the surface is considered to be basic, while for $K_B/K_A < 1$ the surface is considered to be acidic [17].

3 Experimental

3.1 Materials

For the synthesis of the ionic liquid, 1-bromobutane (99%), 1-ethylpiperidine (99%) and acetonitrile were used and were purchased from Sigma Aldrich.

For the IGC analysis, the following solvents were used as probes: n-octane, n-nonane, n-decane, n-undecane, n-dodecane, acetonitrile, n-butanol, pyridine and chloroform. The characteristics of the solvents used for the IGC analysis are presented in Table 1. All solvents were of the highest available purity and were purchased from Sigma Aldrich. Chromosorb W

HP (100/120) mesh was used as the solid support (Antelia, France). All the gases used were purchased from Air Liquide and were of high purity.

Table 1. Physical and chemical properties of the probes used for the IGC analysis [27, 47-52]

Probe	Boiling point (°C)	Saturated vapor pressure (kPa)	α (10^{-19} m^2)	γ_l^d (mJ/m^2)	DN (kJ mol^{-1})	AN^* (kJ mol^{-1})	Character
n-Octane	125.7	1.871	6.29	21.3	n/a	n/a	Neutral
n-Nonane	150.8	0.580	6.89	22.7	n/a	n/a	Neutral
n-Decane	174.2	0.181	7.5	23.4	n/a	n/a	Neutral
n-Undecane	195.9	0.056	8.1	24.6	n/a	n/a	Neutral
n-Dodecane	216.3	0.018	8.7	25.4	n/a	n/a	Neutral
n-Butanol	117.7	0.930	-	-	0	38.1	Acidic
Pyridine	115.3	2.772	-	-	138.6	0.6	Basic
Chloroform	61.2	26.165	-	-	0	22.6	Acidic
Acetonitrile	81.6	12.147	-	-	59	19.7	Amphoteric

3.2 Synthesis and characterization of 1-butyl-1-ethyl piperidinium bromide

1-butyl-1-ethylpiperidinium bromide (Figure 1) was synthesized as previously reported [53]. Briefly, 1-bromobutane was mixed with 1-ethylpiperidine in 100 mL acetonitrile at reflux for 2 days. The solvent was then evaporated using a rotary evaporator. The resulting product appearing as a white solid was washed several times with ethyl acetate. After filtering, the product was initially dried on a rotary evaporator to remove the remaining solvent and then dried under vacuum (~0.1 mbar) for 24 hours. The final product was obtained as a white solid. Purity was checked by Nuclear Magnetic Resonance Spectroscopy (^{1}H NMR). The ^{1}H NMR spectrum was collected on a Bruker WM 400 MHz spectrometer in Dimethysulfoxide (DMSO-d6) as solvent. The spectrum is given in the Supplementary Material section (Figure S1). The chemical shift of different protons from $[C_2C_4PIP]Br$ are at: 3.36-3.30, (6H, m, $(CH_2)_3$-N^+, 3,6), 3.25-3.21, (2H, t, CH_2-N^+, 4), 1.77 (4H, m, 2 CH_2, 2), 1.58-1.53 (4H, m, CH_2, 1,7), 1.37-1.28 (2H, m, CH_2, 8), 1.19-1.15 (3H, t, CH_3, 5), 0.95-0.92 (3H, t, CH_3, 9).

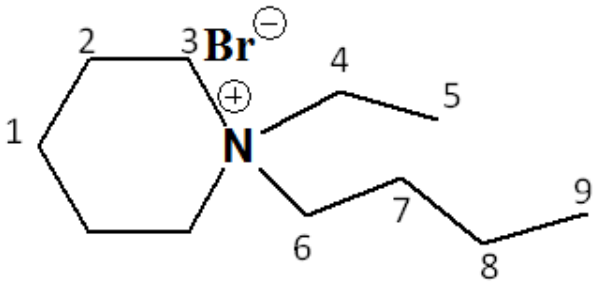

Figure 1. Structure of $[C_2C_4PIP]Br$. The protons observed in the NMR spectrum were identified.

The melting point of $[C_2C_4PIP]Br$ was assessed by Differential Scanning Calorimetry using a TA Instruments DSC 2920 modulated DSC device. The sample was heated from 25°C to 250°C at a heating rate of 5K/min. The DSC thermogram is presented in the Supplementary Material section (Figure S2). The melting point of the $[C_2C_4PIP]Br$ was found to be 140 °C.

3.3 Column preparation and IGC setup

The IGC experiments were performed using a Perkin Elmer Clarus 480 gas chromatograph, equipped with a flame ionization detector (FID). The data acquisition was made with the AZUR software. The retention times of the probes were determined after the calculation of the first-order moment of the concentration distribution. This was necessary due to the slight "tailing" observed at the elution profile of the probes [41]. High purity helium was used as the carrier gas and methane was used as a marker. The flow rate of helium was measured with a soap bubble flowmeter connected to the end of the column, at room temperature. The experiments were performed at infinite dilution, by injecting manually 0.1 μL of each probe with a 1 μL Hamilton syringe. At least three injections of each probe were made and the retention time was taken as the average of the three measurements. The standard deviation was less than 2% in all cases.

The IGC experimental conditions and the column characteristics are presented in Table 2. A stainless steel column was used for the measurements and was washed with acetone prior to use. The stationary phase of the column was prepared via the coating method proposed by Al-Saigh and Munk in order to better control the amount of the salt coated on the solid support [54]. $[C_2C_4PIP]Br$ was coated onto Chromosorb W HP at a loading of 20.7% w/w. The column was preconditioned overnight to the working conditions (temperature and helium flow rate) in order to remove any possible contaminants that could be eluted during measurements.

The protocol regarding the preparation of the column was described in detail elsewhere [50, 55, 56].

Table 2. Chromatographic conditions and column specifications

1-butyl-1-ethylpiperidinium bromide	
Injector temperature (K)	473.15
Detector temperature (K)	473.15
Column temperatures (K)	313.15, 323.15, 333.15, 343.15
Column type of material	SS 316 ASTM A-269
Column length (cm)	70
Column O.D (inch)	1/8
$[C_2C_4PIP]Br$ loading (%)	20.7
Flow rate (mL/min)	10

4 Results

4.1 Dispersive component of the surface energy

The dispersive component of the surface energy of 1-butyl-1-ethylpiperidinium bromide was calculated at the temperature range 313.15-343.15 K, using the Dorris-Gray method and the approach proposed by Schultz.

4.1.1 Dorris-Gray method

The slope of the line obtained when plotting the $RT \ln V_N$ values of *n*-alkanes versus their number of carbon atoms yields the free energy of adsorption of a methylene group, ΔG^{CH_2} as indicated by Eq. (4). The corresponding plot is illustrated in Figure 2. The dispersive component of the surface energy of $[C_2C_4PIP]Br$ was calculated via Eq. (3) according to the Dorris-Gray method. The values of γ_s^d together with their maximum errors are presented in Table 3.

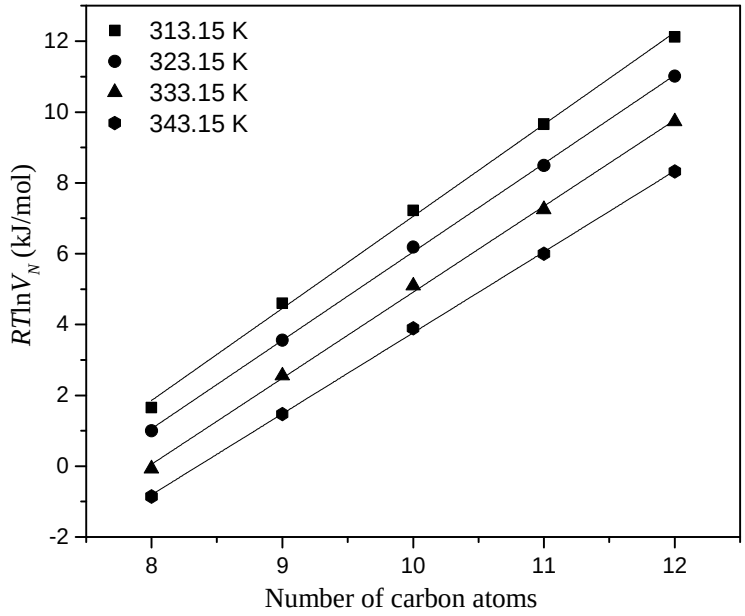

Figure 2. Surface free energy of adsorption of *n*-alkanes $RT\ln V_N$ on [C_2C_4PIP]Br versus their number of carbon atoms, measured at the temperature range 313.15-343.15 K.

4.1.2 Schultz method

Figure 3 illustrates the surface free energy of adsorption of *n*-alkanes $RT\ln V_N$, on [C_2C_4PIP]Br as a function of the term $a\sqrt{\gamma_l^d}$, measured between 313.15 and 343.15 K, according to the Schultz method. The values of the surface area of *n*-alkanes and the values of their dispersive surface energies listed in Table 1 in combination with Eq. (5) were used for this purpose. Results are listed in Table 3.

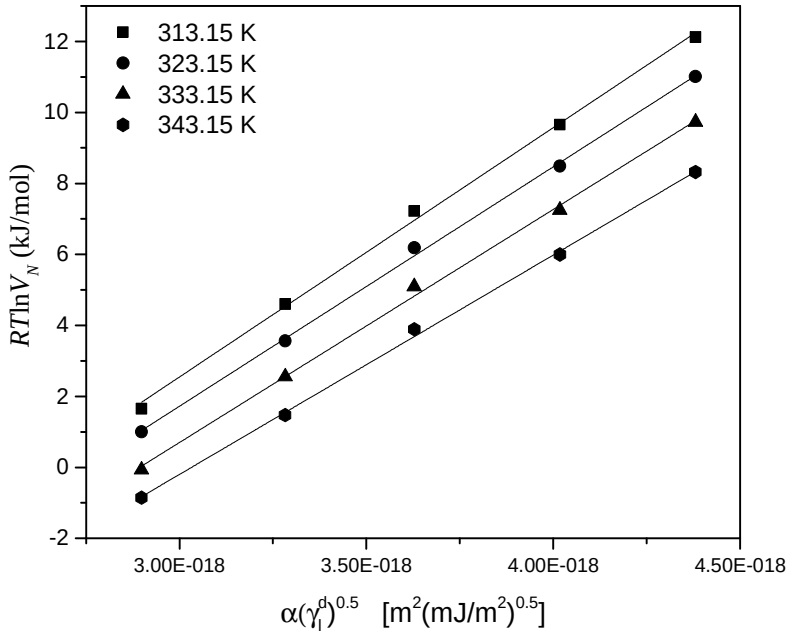

Figure 3. Surface free energy of adsorption of *n*-alkanes $RT\ln V_N$, on $[C_2C_4PIP]Br$ versus $a\sqrt{\gamma_l^d}$ measured at the temperature range 313.15-343.15 K.

Table 3. Dispersive component of the surface energy of $[C_2C_4PIP]Br$ at the temperature range 313.15-343.15 K, obtained by the Dorris-Gray and the Schultz methods

T (K)	Dorris-Gray method		Schultz method	
	γ_s^d (mJ/m^2)	R^2	γ_s^d (mJ/m^2)	R^2
313.15	37.5 ± 1.7	0.998	34.0 ± 1.7	0.998
323.15	35.2 ± 0.8	0.999	31.3 ± 1.2	0.999
333.15	33.9 ± 1.3	0.999	29.7 ± 1.4	0.998
343.15	30.6 ± 0.7	0.999	26.3 ± 1.0	0.999

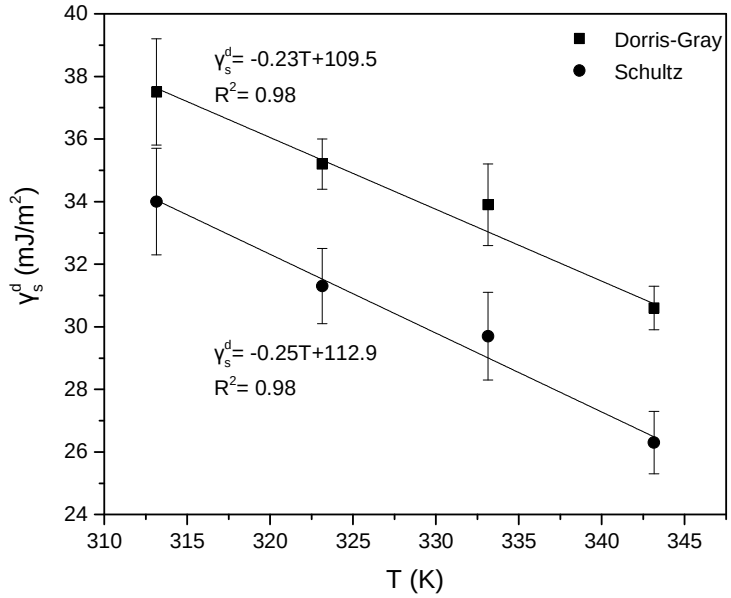

Figure 4. Variation of the dispersive component of the surface energy of $[C_2C_4PIP]Br$ with temperature, at the temperature range 313.15-343.15 K, obtained by the Dorris-Gray and the Schultz methods

Focusing on Figure 2 and Figure 3 we notice that good linearity was achieved for the dependence of the free energy of adsorption with the increasing number of aliphatic carbons (Dorris-Gray method) or with the $a\sqrt{\gamma_l^d}$ term (Schultz method). The dispersive component of the surface energy of $[C_2C_4PIP]Br$ obtained by the Dorris-Gray and the Schultz methods was plotted as a function of temperature (Figure 4) and the values are given in Table 3. For all studied temperatures, high correlation coefficients R^2 values were found. It appears that the dispersive component of the surface energy of $[C_2C_4PIP]Br$ presents a decreasing trend with the increase of temperature [57]. Moreover, based on Figure 4 we notice that the dependence of γ_s^d with temperature is almost linear, and when comparing the slopes corresponding at the descending trend obtained by both methods, we observe that they are similar.

In addition, we notice that the γ_s^d values calculated with the aid of the Dorris-Gray method are higher with respect to those obtained with the Schultz method. The discrepancy between the results calculated by these methods increases with temperature. This trend is in line with the results presented in pertinent literature [58-66].

As it was mentioned in the introduction, there is no study in literature addressing the estimation of the dispersive surface energy of piperidinium or bromide based ILs. However,

the surface tension of piperidinium ILs has been assessed by techniques other than IGC (see Table 4).

Table 4. Surface tension values of piperidinium based ILs taken from literature and dispersive component of the surface energy results of $[C_2C_4PIP]Br$ of the present study

T (K)	γ (mJ/m^2)		γ_s^d (mJ/m^2)
	$[C_3C_1PIP][NTf_2]$	$[C_4C_1PIP][NTf_2]$ [68]	$[C_2C_4PIP]Br$ (this work)
298	35.2 [69] / 35.3 [68]	34.2	-
303.2	34.5 [67] / 35.1 [68]	34.0	-
313.2	34.5 [68]	33.5	34.0 - 37.5
323.2	34.0 [68]	33.0	31.3 - 35.2
333.2	33.5 [68]	32.5	29.7 - 34.0
343.2	33.0 [68]	32.1	26.3 - 30.6

Osada et al. [67] reported the surface energy of 1-methyl-1-propylpiperidinium bis(trifluoromethanesulfonyl)imide ($[C_3C_1PIP][NTf_2]$) measured with the Dynamic Light Scattering (DLS) technique. Bhattacharjee et al. [68] assessed the surface energy of $[C_3C_1PIP][NTf_2]$ and $[C_4C_1PIP][NTf_2]$ (1-Butyl-1-methylpiperidinium bis (trifluoromethyl sulfonyl)imide) by using the contact angle method. The comparison between our results (last column in Table 4) with literature data is not straightforward for several reasons; firstly, the latter concern surface energy values contrary to the former which concern values of dispersive surface energy. Furthermore, as it has been shown, the measuring techniques of the surface energy as well as the sample purity have an impact on the values of γ [16, 68]. Moreover, the anion $[NTf_2]^-$ ((bistrifluoromethanesulfonyl)imide) reported in the literature is a polyatomic, bulky and very weakly coordinating anion. It is thus very different from the small and coordinating bromide ion studied here. On these grounds, only a rough comparison between literature data and the results of this study can be made. As a first remark, the same temperature dependence of γ and is γ_s^d observed for all ILs, all values decrease with increasing temperature. It is well known that the surface tension depends on the contribution of the groups which are exposed at the surface [16, 68]. In the case of ionic liquids, when the cation bears long alkyl side chains and is thus bulkier than the anion, the surface tension is affected primarily by the nature of the cation [16, 68].

4.2 Acid-base interactions

The ability of the ionic liquid to intermolecular specific interactions with other substances is strongly dependent on the presence of acidic and basic sites on its surface.

The assessment of the acid-base interactions of a surface includes the calculation of the specific component of the free energy of adsorption of a probe, ΔG^{sp}, the specific component of the free enthalpy of adsorption of a probe, ΔH^{sp} and the ratio K_B/K_A of the examined surface [17]. As it has been mentioned in Section 2.2, several methods have been developed for the acid-base characterisation of a material through the use of the IGC technique. The Schultz method allows the estimation of ΔG^{sp} through the use of the term $\sqrt{\gamma_l^d}$, whereas the Papirer method and the Brookman and Sawyer method are based on the saturated vapor pressures and the boiling points of the probes, respectively. The latter two properties are readily available in literature, contrary to the molecular area and the dispersive component of the surface tension of polar probes. The discrepancy between the values of γ_s^d and a of polar probes appearing in literature [65, 70] is due to the presence of one or more functional groups [59]. For the above reasons, although in the present study the Schultz method was employed for the dispersive surface energy calculation of $[C_2C_4PIP]Br$, the acid-base interactions were studied with the aid of the Flour and Papirer method and the Brookman and Sawyer method.

4.2.1 Flour and Papirer method

Figure 5 presents the results of the energies of adsorption of *n*-alkanes and polar probes on the surface of $[C_2C_4PIP]Br$ versus the logarithm of their saturated vapour pressure, according to the Flour and Papirer method. The straight reference line defines the London dispersive interactions, while the energies of adsorption polar probes lie above this line.

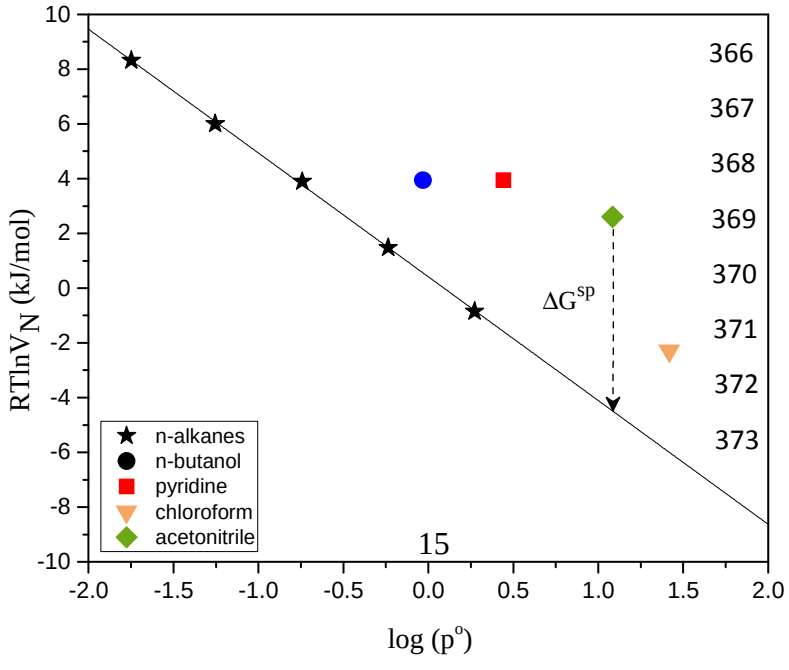

Figure 5. Energy of adsorption of *n*-alkanes and polar probes on the surface of $[C_2C_4PIP]Br$ versus the logarithm of their saturated vapour pressure, at 343.15 K.

The values of the specific component of the free energy of adsorption ΔG^{sp} of the polar probes used in this study are high. The fact that the ΔG^{sp} values of the Lewis acidic, basic, and amphoteric probes lie above the reference line of *n*-alkanes suggests that all types of active sites are present on the surface of $[C_2C_4PIP]Br$ [71]. The highest ΔG^{sp} values, correspond to acetonitrile, which has an amphoteric character.

4.2.2 Brookman and Sawyer method

The contribution of specific interactions to the free energy of adsorption ΔG^{sp} of polar probes, was calculated by the aid of the Brookman and Sawyer method, as shown in Figure 6.

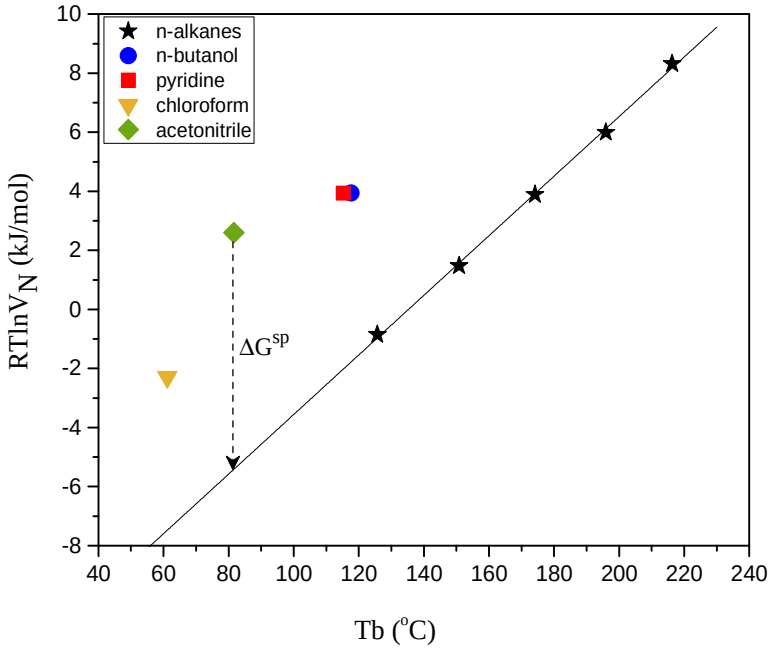

Figure 6. Energy of adsorption of *n*-alkanes and polar probes on the surface of $[C_2C_4PIP]Br$ versus their boiling temperatures, at 343.15 K.

The ΔG^{sp} values obtained by both methods exhibit the same trend. Similarly to the conclusion extracted by the Flour and Papirer analysis, results show that both acidic and basic sites exist on the surface of $[C_2C_4PIP]Br$. However, the dominant character of the surface is determined by means of the K_B/K_A ratio.

For such an estimation, the values of the enthalpy and entropy of adsorption of polar probes on the surface of $[C_2C_4PIP]Br$ were calculated by the aid of Eq. (7) and via a plot of ΔG^{sp}

values versus the reciprocal temperature, T^{-1}. The results obtained by both methods employed are reported in Table 5.

Table 5. Specific components of the enthalpy and entropy of adsorption of polar probes on the surface of $[C_2C_4PIP]Br$ at the temperature range 313.15-343.15 K

Probe	Flour and Papirer method		Brookman and Sawyer method	
	$-\Delta H^{sp}$ (kJ/mol)	$-\Delta S^{sp}$ (J/mol K)	$-\Delta H^{sp}$ (kJ/mol)	$-\Delta S^{sp}$ (kJ/mol K)
n-Butanol	5.59	6.48	11.31	15.56
Pyridine	7.74	6.51	9.30	8.99
Chloroform	24.07	59.58	28.73	66.41
Acetonitrile	0.63	-18.48	3.55	-13.84

The enthalpies and entropies of adsorption of polar probes on the surface of $[C_2C_4PIP]Br$ estimated with the Flour and the Brookman methods are comparable, with the exception of n-butanol. The enthalpy of adsorption of all probes was found to be exothermic in all cases. Acetonitrile which is an amphoteric probe presents the highest enthalpy of adsorption whereas chloroform which is acidic has the lowest ΔH^{sp} implying that $[C_2C_4PIP]Br$ is amphoteric with a basic character. The values of the specific components of the entropy of adsorption of polar probes on the surface of $[C_2C_4PIP]Br$ follow the same trend as discussed above. Acetonitrile has the highest ΔS^{sp} values, indicating that the surface is amphoteric. Moreover, we notice that all ΔS^{sp} values are negative, with the exception of acetonitrile. The adsorption of a probe from a surface is usually accompanied by an entropy loss as the probe passes from the less ordered vapor phase to the more ordered adsorbed phase. In the case of acetonitrile, the entropy increase implies an increase in the degrees of freedom which could be attributed to the rearrangement of the surface [72].

4.2.3 Acidity and basicity constants

The values for the specific enthalpies of polar probes were employed in order to evaluate the acidity and basicity constants of $[C_2C_4PIP]Br$. According to Eq. (8) the K_A and K_B constants can be assessed by the slope and the intercept, respectively, of a plot of $\Delta H^{sp}/AN^*$ versus DN/AN^*. Based on the values of the Gutmann's donor and modified acceptor numbers of the polar probes presented in Table 1 as well as the values of ΔH^{sp} obtained by the two methods used, K_A and K_B constants were evaluated (Figures 7 and 8). Examining the two plots we can

deduce that, in both cases, linear dependencies of $\Delta H^{sp}/AN^{*}$versus DN/AN^{*} were achieved, based on the high values of the regression coefficients. Similar plots for the estimation of the K_A and K_B constants appear in literature [27, 51, 62, 68]. The results of the acidity and basicity constants of the surface of $[C_2C_4PIP]Br$ are reported in Table 6.

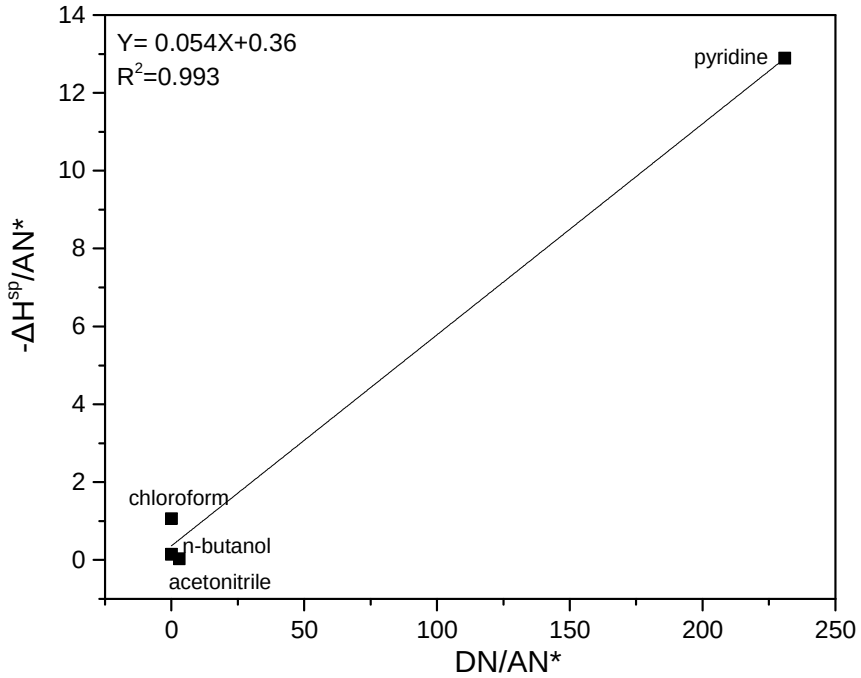

Figure 7. Determination of the K_A and K_B values of the of $[C_2C_4PIP]Br$ based on the Flour and Papirer approach.

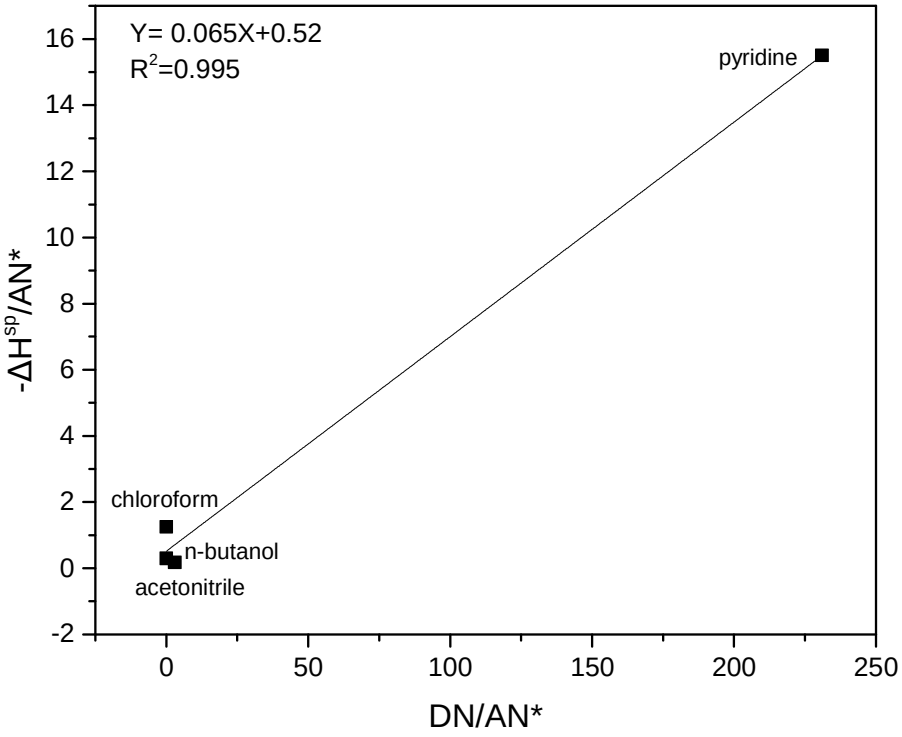

Figure 8. Determination of the K_A and K_B values of the of $[C_2C_4PIP]Br$ based on the Brookman and Sawyer method.

Table 6. Acidity and basicity constants of the surface of $[C_2C_4PIP]Br$

Method	K_A	K_B	K_B/K_A
Flour and Papirer	0.054	0.36	6.67
Brookman and Sawyer	0.065	0.52	8.00

The K_B/K_A ratios calculated by the Flour and Papirer method and the Brookman and Sawyer method suggest that the surface of 1-butyl-1-ethylpiperidinium bromide has a predominantly Lewis basic character. This conclusion is in line with the findings of the analysis based on the values of the energy and enthalpy of polar probes, presented in paragraphs 4.2.1 and 4.2.2. Despite the fact that the K_B/K_A ratios are not similar, we can safely conclude that $[C_2C_4PIP]Br$ is a Lewis base, since in both cases the K_B/K_A ratio is greater than 1.

Bearing in mind the structure of 1-butyl-1-ethylpiperidinium bromide, we notice that both acidic and basic moieties are present in the molecule. As no comparable work has been carried out previously for solid organic salts or ionic liquids below their melting point, neither the comparison with literature nor the interpretation of our results are straightforward.

Nevertheless, a tentative explanation can be given as following. Since in our case, the ions of the salt are relatively small and bound together, the overall basicity of $[C_2C_4PIP]Br$ is due to an average of all of its parts, i.e. the alkyl groups, the positive charge on the nitrogen atom and the Br^- anion. As reported previously in IGC studies dealing with polymers, CH_2 and CH_3 groups are known to be weak Lewis acidic sites [50, 72, 73]. On the other hand, Br^-, as F^- or Cl^- anions, is a dense, monoatomic and relatively electronegative anion, and is known to be basic [50, 74]. The positive charge on the nitrogen is acidic, but is expected to be hidden and to be sterically hindered by the alkyl groups bound to it. Therefore, we can surmise that the general basic character of $[C_2C_4PIP]Br$ is due to the relatively dense and monoatomic bromide anion.

Conclusions

This contribution reports for the first time on the surface characterization of a piperidinium based organic salt, 1-butyl-1-ethylpiperidinium bromide, by means of IGC. Measurements were conducted at a temperature range (313.15-343.15 K), well below the melting point of $[C_2C_4PIP]Br$ (413.15 K) to ensure that the dominant retention mechanism of the probes is adsorption onto the surface. The Schultz and the Dorris-Gray methods were used for the calculation of the dispersive component of the surface energy. Results showed that γ_s^d decreases with temperature. Moreover, the comparison of the dispersive component of the surface energy of $[C_2C_4PIP]Br$ with that of two piperidinium based ILs revealed that the results of this study are comparable with literature values. The anion does therefore not appear to play a crucial role in the surface energy of the piperidnium-based organic salts studied here and in the literature. The acid/base characterization based on the Flour and Papirer approach and the Brookman and Sawyer method showed that the surface of $[C_2C_4PIP]Br$ is amphoteric with a predominantely basic character, a conclusion which is further supported by taking into account the molecular structure of $[C_2C_4PIP]Br$ bearing, both, weak Lewis acidic and basic sites.

Acknowledgments

The authors acknowledge Grenoble INP for post-doctoral fellowship for S.P. and financial support for this project.

References

[1] S. Genand-Pinaz, N. Papaiconomou, J.-M. Leveque, Removal of platinum from water by precipitation or liquid-liquid extraction and separation from gold using ionic liquids, Green Chem. 15 (2013) 2493-2501.

[2] T.M. Koller, C. Steininger, M.H. Rausch, A.P. Fröba, A Simple Prediction Method for the Surface Tension of Ionic Liquids as a Function of Temperature, Int. J.Thermophys. 38 (2017) 167.

[3] T. Mandai, K. Yoshida, K. Ueno, K. Dokko, M. Watanabe, Criteria for solvate ionic liquids, Phys. Chem. Chem. Phys. 16 (2014) 8761-8772.

[4] V. Mazan, I. Billard, N. Papaiconomou, Experimental connections between aqueous-aqueous and aqueous-ionic liquid biphasic systems, RSC Adv. 4 (2014) 13371-13384.

[5] P. Pollet, E.A. Davey, E.E. Urena-Benavides, C.A. Eckert, C.L. Liotta, Solvents for sustainable chemical processes, Green Chem. 16 (2014) 1034-1055.

[6] F. Pena-Pereira, A. Kloskowski, J. Namiesnik, Perspectives on the replacement of harmful organic solvents in analytical methodologies: a framework toward the implementation of a generation of eco-friendly alternatives, Green Chem. 17 (2015) 3687-3705.

[7] H.F. Almeida, A.R.R. Teles, J.A. Lopes-da-Silva, M.G. Freire, J.A. Coutinho, Influence of the anion on the surface tension of 1-ethyl-3-methylimidazolium-based ionic liquids, J. Chem. Thermodyn. 54 (2012) 49-54.

[8] L. Deng, Q. Wang, Y. Chen, Z. Zhang, J. Tang, Determination of the solubility parameter of ionic liquid 1-octyl-3-methylimidazolium hexafluorophosphate by inverse gas chromatography, J. Mol. Liq. 187 (2013) 246-251.

[9] M. Shukla, S. Saha, A Comparative Study of Piperidinium and Imidazolium Based Ionic Liquids: Thermal, Spectroscopic and Theoretical Studies, in: Ionic Liquids-New Aspects for the Future INTECH Open Access Publisher, 2013.

[10] M. Shukla, H. Noothalapati, S. Shigeto, S. Saha, Importance of weak interactions and conformational equilibrium in N-butyl-N-methylpiperidinium bis (trifluro-methanesulfonyl) imide room temperature ionic liquids: Vibrational and theoretical studies, Vib. Spectrosc. 75 (2014) 107-117.

[11] G. Járvás, J. Kontos, G. Babics, A. Dallos, A novel method for the surface tension estimation of ionic liquids based on COSMO-RS theory, Fluid Phase Equilib. 468 (2018) 9-17.

509 [12] T.M. Koller, M.H. Rausch, K. Pohako-Esko, P. Wasserscheid, A.P. Fröba, Surface
510 tension of tricyanomethanide-and tetracyanoborate-based imidazolium ionic liquids by
511 using the pendant drop method, J. Chem. Eng. Data 60 (2015) 2665-2673.
512 [13] G. Law, P.R. Watson, Surface tension measurements of N-alkylimidazolium ionic
513 liquids, Langmuir, 17 (2001) 6138-6141.
514 [14] S.A. Mirkhani, F. Gharagheizi, N. Farahani, K. Tumba, Prediction of surface tension of
515 ionic liquids by molecular approach, J. Mol. Liq. 179 (2013) 78-87.
516 [15] J. Restolho, J.L. Mata, B. Saramago, On the interfacial behavior of ionic liquids:
517 Surface tensions and contact angles, J. Colloid Interf. Sci. 340 (2009) 82-86.
518 [16] M. Tariq, M.G. Freire, B. Saramago, J.A. Coutinho, J.N.C. Lopes, L.P.N. Rebelo,
519 Surface tension of ionic liquids and ionic liquid solutions, Chem. Soc. Rev. 41 (2012)
520 829-868.
521 [17] A. Voelkel, B. Strzemiecka, K. Adamska, K. Milczewska, Inverse gas chromatography
522 as a source of physiochemical data, J. Chromatogr. A 1216 (2009) 1551-1566.
523 [18] Y. Chen, Q. Wang, Z. Zhang, J. Tang, Determination of the Solubility Parameter of
524 Ionic Liquid 1-Hexyl-3-methylimidazolium Hexafluorophosphate by Inverse Gas
525 Chromatography, Ind. Eng. Chem. Res. 51 (2012) 15293-15298.
526 [19] U. Domańska, A. Marciniak, Measurements of activity coefficients at infinite dilution
527 of aromatic and aliphatic hydrocarbons, alcohols, and water in the new ionic liquid
528 [EMIM][SCN] using GLC, J. Chem. Thermodyn. 40 (2008) 860-866.
529 [20] K. Heydar, M. Nazifi, A. Sharifi, M. Mirzaei, H. Gharavi, S. Ahmadi, Determination of
530 Activity Coefficients at Infinite Dilution of Solutes in New Dicationic Ionic Liquids
531 Based on Morpholine Using Gas–Liquid Chromatography, Chromatographia, 76 (2013)
532 165-175.
533 [21] M. Królikowski, M. Królikowska, The study of activity coefficients at infinite dilution
534 for organic solutes and water in 1-butyl-4-methylpyridinium dicyanamide,
535 [B4MPy][DCA] using GLC, J. Chem. Thermodyn. 68 (2014) 138-144.
536 [22] A. Marciniak, M. Wlazło, Activity Coefficients at Infinite Dilution Measurements for
537 Organic Solutes and Water in the Ionic Liquid 1-(3-Hydroxypropyl)pyridinium
538 Trifluorotris(perfluoroethyl)phosphate, J. Phys. Chem. B 114 (2010) 6990-6994.
539 [23] A. Marciniak, M. Wlazło, Activity coefficients at infinite dilution and physicochemical
540 properties for organic solutes and water in the ionic liquid 1-(2-methoxyethyl)-1-
541 methylpiperidinium bis(trifluoromethylsulfonyl)-amide, J. Chem. Thermodyn. 49
542 (2012) 137-145.

[24] F. Mutelet, J.-N. Jaubert, Accurate measurements of thermodynamic properties of solutes in ionic liquids using inverse gas chromatography, J. Chromatogr. A 1102 (2006) 256-267.

[25] F. Mutelet, J.-N. Jaubert, Measurement of activity coefficients at infinite dilution in 1-hexadecyl-3-methylimidazolium tetrafluoroborate ionic liquid, J. Chem. Thermodyn. 39 (2007) 1144-1150.

[26] Q. Wang, Y. Chen, L. Deng, J. Tang, Z. Zhang, Determination of the solubility parameter of ionic liquid 1-allyl-3-methylimidazolium chloride by inverse gas chromatography, J. Mol. Liq. 180 (2013) 135-138.

[27] Q. Wang, Y. Chen, Z. Zhang, J. Tang, Determination of Surface Characteristics of Ionic Liquid [1-Hexyl-3-methylimidazolium Hexafluorophosphate] by Inverse Gas Chromatography, J. Chem. Eng. Data 58 (2013) 2142-2146.

[28] Y. Chen, Q. Wang, L. Deng, Z. Zhang, J. Tang, Characterization of surface properties of 1-allyl-3-methylimidazolium chloride ionic liquid by inverse gas chromatography, Chin. J. Chromatogr. 31 (2013) 147-150.

[29] T. Ban, X.-P. Li, C.-L. Li, Q. Wang, Surface Characterization of a Series of 1-Alkyl-3-methylimidazolium-Based Ionic Liquids by Inverse Gas Chromatography, Ind. Eng. Chem. Res. 57 (2018) 12249-12253.

[30] X. Li, Q. Wang, L. Li, Y. Ding, Determination of the thermodynamic parameters of ionic liquid 1- hexyl- 3□methylimidazolium tetrafluoroborate by inverse gas chromatography, Chin. J. Chromatogr. 33 (2015) 58-64.

[31] X. Li, Q. Wang, L. Li, L. Deng, Z. Zhang, L. Tian, Determination of the thermodynamic parameters of ionic liquid 1-hexyl-3-methylimidazolium chloride by inverse gas chromatography, J. Mol. Liq. 200 (2014) 139-144.

[32] L. Deng, Q. Wang, Z. Zhang, J. Tang, Determination of thermodynamic parameters for ionic liquid 1-hexyl-3-methylimidazolium trifluoromethansulfonate by inverse gas chromatography, Chin. J. Chromatogr. 32 (2014) 169-173.

[33] L. Tian, Y. Chen, Q. Wang, Chin. J. Appl. Chem. 34 (2017) 824-832.

[34] S. Zhang, X. Lu, Q. Zhou, X. Li, X. Zhang, S. Li, Ionic Liquids: Physicochemical Properties, Elsevier, Amsterdam, 2009.

[35] U. Domańska, M. Królikowska, K. Paduszyński, Physico-chemical properties and phase behaviour of piperidinium-based ionic liquids, Fluid Phase Equilib. 303 (2011) 1-9.

[36] U. Domańska, K. Paduszyński, Measurements of activity coefficients at infinite dilution of organic solutes and water in 1-propyl-1-methylpiperidinium bis {(trifluoromethyl) sulfonyl}imide ionic liquid using g.l.c, J. Chem. Thermodyn. 42 (2010) 1361-1366.

[37] A. Marciniak, M. Wlazło, Activity coefficients at infinite dilution and physicochemical properties for organic solutes and water in the ionic liquid 1-(2-methoxyethyl)-1-methylpiperidinium trifluorotris(perfluoroethyl)phosphate, J. Chem. Thermodyn. 57 (2013) 197-202.

[38] K. Paduszyński, U. Domańska, Limiting Activity Coefficients and Gas–Liquid Partition Coefficients of Various Solutes in Piperidinium Ionic Liquids: Measurements and LSER Calculations, J. Phys. Chem. B 115 (2011) 8207-8215.

[39] M.N. Belgacem, G. Czeremuszkin, S. Sapieha, A. Gandini, Surface characterization of cellulose fibres by XPS and inverse gas chromatography, Cellulose, 2 (1995) 145-157.

[40] J. Kolodziejek, A. Voelkel, K. Heberger, Characterization of hybrid materials by means of inverse gas chromatography and chemometrics, J. Pharm. Sci. 102 (2013) 1524-1531.

[41] J.R. Conder, C.L. Young, Physicochemical Measurement by Gas Chromatography, Wiley, New York, 1979.

[42] J. Schultz, L. Lavielle, C. Martin, The role of the interface in carbon fibre-epoxy composites, J. Adhesion, 23 (1987) 45-60.

[43] C. Saint Flour, E. Papirer, Gas-solid chromatography: a quick method of estimating surface free energy variations induced by the treatment of short glass fibers, J. Colloid Interf. Sci. 91 (1983) 69-75.

[44] D.J. Brookman, D.T. Sawyer, Specific Interactions Affecting Gas Chromatographic Retention for Modified Alumina Columns, Anal. Chem. 40 (1968) 106-110.

[45] V. Gutmann, The Donor-Acceptor Approach to Molecular Interactions, Plenum Press, New York, 1978.

[46] D.P. Kamdem, S.K. Bose, P. Luner, Inverse Gas-Chromatography Characterization of Birch Wood Meal, Langmuir, 9 (1993) 3039-3044.

[47] F.L. Riddle, F.M. Fowkes, Spectral Shifts in Acid-Base Chemistry .1. Vanderwaals Contributions to Acceptor Numbers, J. Am. Chem. Soc. 112 (1990) 3259-3264.

[48] D. Cava, R. Gavara, J. Lagaron, A. Voelkel, Surface characterization of poly (lactic acid) and polycaprolactone by inverse gas chromatography, J. Chromatogr. A 1148 (2007) 86-91.

[49] T.E. Daubert, R.P. Danner, Physical and Thermodynamic Properties of Pure Chemicals: Data Compilation, Hemisphere, New York, 2001.

609 [50] S.K. Papadopoulou, G. Dritsas, I. Karapanagiotis, I. Zuburtikudis, C. Panayiotou,
610 Surface characterization of poly (2, 2, 3, 3, 3-pentafluoropropyl methacrylate) by
611 inverse gas chromatography and contact angle measurements, Eur. Polym. J. 46 (2010)
612 202-208.
613 [51] J.M.R.C.A. Santos, J.T. Guthrie, Lewis acid/base character and crystallisation properties
614 of poly(butylene terephthalate), J. Chromatogr. A 1379 (2015) 92-99.
615 [52] K. Vasanth Kumar, F. Rocha, On the effect of a non-ionic surfactant on the surface of
616 sucrose crystals and on the crystal growth process by inverse gas chromatography, J.
617 Chromatogr. A 1216 (2009) 8528-8534.
618 [53] N. Papaiconomou, J. Estager, Y. Traore, P. Bauduin, C. Bas, S. Legeai, S. Viboud, M.
619 Draye, Synthesis, Physicochemical Properties, and Toxicity Data of New Hydrophobic
620 Ionic Liquids Containing Dimethylpyridinium and Trimethylpyridinium Cations†, J.
621 Chem. Eng. Data 55 (2010) 1971-1979.
622 [54] Z.Y. Al-Saigh, P. Munk, Study of polymer-polymer interaction coefficients in polymer
623 blends using inverse gas chromatography, Macromolecules, 17 (1984) 803-809.
624 [55] S.K. Papadopoulou, C. Panayiotou, Assessment of the thermodynamic properties of
625 poly(2,2,2-trifluoroethyl methacrylate) by inverse gas chromatography, J. Chromatogr.
626 A 1324 (2014) 207-214.
627 [56] S.K. Papadopoulou, I. Karapanagiotis, I. Zuburtikudis, C. Panayiotou, Thermodynamic
628 characterization of poly(2,2,3,3,3-pentafluoropropyl methacrylate), J. Polym. Sci. Pol.
629 Phys. 48 (2010) 1826-1833.
630 [57] S. Ramanaiah, V. Karde, P. Venkateswarlu, C. Ghoroi, Effect of temperature on the
631 surface free energy and acid–base properties of Gabapentin and Pregabalin drugs − a
632 comparative study, RSC Adv. 5 (2015) 48712-48719.
633 [58] A. Voelkel, K. Batko, K. Adamska, B. Strzemiecka, Determination of Hansen solubility
634 parameters by means of gas-solid inverse gas chromatography, Adsorpt. Sci. Technol.
635 26 (2008) 93-102.
636 [59] A. van Asten, N. van Veenendaal, S. Koster, Surface characterization of industrial fibers
637 with inverse gas chromatography, J. Chromatogr. A 888 (2000) 175-196.
638 [60] B. Shi, Y. Wang, L. Jia, Comparison of Dorris–Gray and Schultz methods for the
639 calculation of surface dispersive free energy by inverse gas chromatography, J.
640 Chromatogr. A 1218 (2011) 860-862.

[61] L.H.G.J. Segeren, M.E.L. Wouters, M. Bos, J.W.A. van den Berg, G.J. Vancso, Surface energy characteristics of toner particles by automated inverse gas chromatography, J. Chromatogr. A 969 (2002) 215-227.

[62] H. Ocak, S. Mutlu-Yanic, F. Cakar, B. Bilgin-Eran, D. Guzeller, F. Karaman, O. Cankurtaran, A study of the thermodynamical interactions with solvents and surface characterisation of liquid crystalline 5-((S)-3,7-dimethyloctyloxy)-2-[[[4-(dodecyloxy)phenyl]imino]-methyl]phenol by inverse gas chromatography, J. Mol. Liq. 223 (2016) 861-867.

[63] M.A. Mohammad, Chromatographic adhesion law to simplify surface energy calculation, J. Chromatogr. A 1318 (2013) 270-275.

[64] L. Lapčík, M. Otyepka, E. Otyepková, B. Lapčíková, R. Gabriel, A. Gavenda, B. Prudilová, Surface heterogeneity: Information from inverse gas chromatography and application to model pharmaceutical substances, Curr. Opin. Colloid In. 24 (2016) 64-71.

[65] J.A.F. Gamelas, E. Ferraz, F. Rocha, An insight into the surface properties of calcined kaolinitic clays: The grinding effect, Colloid. Surface. A 455 (2014) 49-57.

[66] C. Bilgiç, F. Tümsek, Determination of the acid/base properties of MgY and NH4Y molecular sieves by inverse gas chromatography, J. Chromatogr. A 1162 (2007) 83-89.

[67] R. Osada, T. Hoshino, K. Okada, Y. Ohmasa, M. Yao, Surface tension of room temperature ionic liquids measured by dynamic light scattering, J. Chem. Phys. 130 (2009) 184705.

[68] A. Bhattacharjee, P.J. Carvalho, J.A. Coutinho, The effect of the cation aromaticity upon the thermophysical properties of piperidinium-and pyridinium-based ionic liquids, Fluid Phase Equilib. 375 (2014) 80-88.

[69] M. Oliveira, M. Dominguez-Perez, O. Cabeza, J. Lopes-da-Silva, M. Freire, J. Coutinho, Surface tensions of binary mixtures of ionic liquids with bis (trifluoromethylsulfonyl) imide as the common anion, J. Chem. Thermodyn. 64 (2013) 22-27.

[70] M.N. Belgacem, A. Gandini, in: E. Pefferkorn (Ed.), Interfacial Phenomena in Chromatography, Marcel Dekker Inc., New York, 1999.

[71] A.B. Nastasović, A.E. Onjia, S.K. Milonjić, S.M. Jovanović, Surface characterization of macroporous glycidyl methacrylate based copolymers by inverse gas chromatography, Eur. Polym. J. 41 (2005) 1234-1242.

[72] J. Santos, K. Fagelman, J. Guthrie, Characterisation of the surface Lewis acid–base properties of the components of pigmented, impact-modified, bisphenol A polycarbonate–poly (butylene terephthalate) blends by inverse gas chromatography–phase separation and phase preferences, J. Chromatogr. A 969 (2002) 119-132.

[73] J.M.R.C.A. Santos, J.T. Guthrie, Study of a core-shell type impact modifier by inverse gas chromatography, J. Chromatogr. A 1070 (2005) 147-154.

[74] M.-L. Abel, M.M. Chehimi, F. Fricker, M. Delamar, A.M. Brown, J.F. Watts, Adsorption of poly(methyl methacrylate) and poly(vinyl chloride) blends onto polypyrrole: Study by X-ray photoelectron spectroscopy, time-of-flight static secondary ion mass spectroscopy, and inverse gas chromatography, J. Chromatogr. A 969 (2002) 273-285.